

Article

# Excited-state dynamics of room-temperature phosphorescent organic materials based on monobenzil and bisbenzil frameworks

Kaveendra Maduwantha<sup>1,2</sup>, Shigeyuki Yamada<sup>3</sup>, Kaveenga Rasika Koswattage<sup>2,4</sup>, Tsutomu Konno<sup>3</sup> and Takuya Hosokai<sup>2,\*</sup>

<sup>1</sup> Faculty of Graduate Studies, Sabaragamuwa University of Sri Lanka, P.O. Box 02, Belihuloya 70140, Sri Lanka

<sup>2</sup> National Metrology Institute of Japan, National Institute of Advanced Industrial Science and Technology, 1-1-1 Umezono, Tsukuba 305-8565, Japan

<sup>3</sup> Faculty of Molecular Chemistry and Engineering, Kyoto Institute of Technology, Matsugasaki, Sakyo-ku, Kyoto 606-8585, Japan

<sup>4</sup> Faculty of Technology, Sabaragamuwa University of Sri Lanka, P.O. Box 02, Belihuloya 70140, Sri Lanka.

\* Correspondence: e-mail@e-mail.com; Tel.: (optional; include country code; if there are multiple corresponding authors: [t.hosokai@aist.go.jp](mailto:t.hosokai@aist.go.jp); +81-29-861-1424 (T.H.)

**Abstract:** Room-temperature phosphorescent (RTP) materials have been attracted tremendous interest owing to their unique material characteristics and potential applications for state-of-the-art optoelectronic devices. Recently, we have reported a synthesis and fundamental photophysical properties of new RTP materials based on benzil, i.e., fluorinated monobenzil derivative and fluorinated and non-fluorinated bisbenzil derivative analogues [Yamada, S. et al, *Beilstein J. Org. Chem.* 2020, 16, 1154–1162.]. To further understand their RTP properties, here we investigated the excited-state dynamics and photostability of the derivatives by means of time-resolved and steady-state photoluminescence spectroscopies. For these derivatives, clear RTP emissions with lifetimes on the microsecond timescale were identified. Among them, the monobenzil derivative was found to be the most efficient RTP material, showing both the longest lifetime and highest amplitude RTP emission. Time-resolved photoluminescence spectra measured at 77 K and density functional theory calculations revealed the existence of a second excited triplet state in the vicinity of the first excited singlet state for the monobenzil derivative, indicative of the presence of a fast intersystem crossing pathway. A discussion of the correlation between the excited state dynamics, emission properties, and conformational flexibility of the three derivatives is presented.

**Keywords:** Room temperature phosphorescence; organic molecule; Excited state dynamics; Time-resolved photoluminescence spectroscopy; Photostability

## 1. Introduction

In the last decade, room-temperature phosphorescent (RTP) materials have drawn an intense interest owing to their potential uses in medical applications, such as bio-imaging; security applications, including security inks for information encryption and anticounterfeiting measures; as photosensitizers; for emergency signage; for geochemical dating; in advanced turbo-machinery; for oxygen measurements inside and outside living organisms; and for electronic applications, such as data storage, logic gates and organic light-emitting diodes (OLEDs) [1–7]. Thus far, heavy-metal-based inorganic compounds and organometallic materials have proven to be the most efficient RTP materials. For instance, tris[2-phenylpyridinato-*C*<sup>2</sup>,*N*]iridium(III) has been reported to have a high RTP quantum yield and has been investigated for use as a highly efficient green light emitter in OLEDs [1]. Because of the heavy metal effect, the spin–orbit coupling (SOC) is increased, increasing

the rate of the spin-flip processes from the first excited singlet state ( $S_1$ ) to the first excited triplet state ( $T_1$ ) (i.e., the intersystem crossing (ISC)) and from  $T_1$  to the ground state ( $S_0$ ) with radiative emission (i.e., phosphorescence). However, there are major drawbacks in RTP materials containing heavy metals, including high costs, limited resources, and high toxicity. Hence, metal-free organic materials that can replace RTP materials containing heavy metals are in demand.

Since the first observation of the room-temperature afterglow of the metal-free organic luminophore carbazole in crystalline form in 1978 by Bilen et al., the search for efficient metal-free RTP materials and their applications has drawn significant interest [8–15]. An important RTP molecule is benzil, an  $\alpha$ -dicarbonyl (a molecule with two carbonyl (C=O) groups on neighbouring carbon atoms). Similar to the heavy-metal effect, the incorporation of carbonyl groups in organic molecules tends to induce a greater SOC by lowering the  $S_1$ - $T_1$  energy gap according to the orbital selection rule between the initial and final state upon photoexcitation, that is, the El-Sayed rules [16, 17]. Benzil, benzil derivatives, and dicarbonyl compounds (Figure 1) have been reported to emit either RTP or phosphorescence at liquid nitrogen temperature [17–24]. Among these compounds, benzil has been the subject of extensive investigations in the field of photochemistry because conformational changes upon photoexcitation have been reported [16, 22, 23, 25–27]. Benzil in  $S_0$  has a twisted geometry, and, upon photoexcitation, the geometry reorients into a trans-planar (TP) geometry. Benzil in the TP geometry is reported to emit light from both excited singlet and triplet states. The conformational flexibility is known to enhance the SOC because of the twisting around the bond between the two carbonyl groups [16]. As a result, benzil shows efficient ISC with a high quantum yield of 0.92 (in solid form) [28]. Thus, in this study, we investigated the photochemistry of novel derivatives based on the benzil structure.

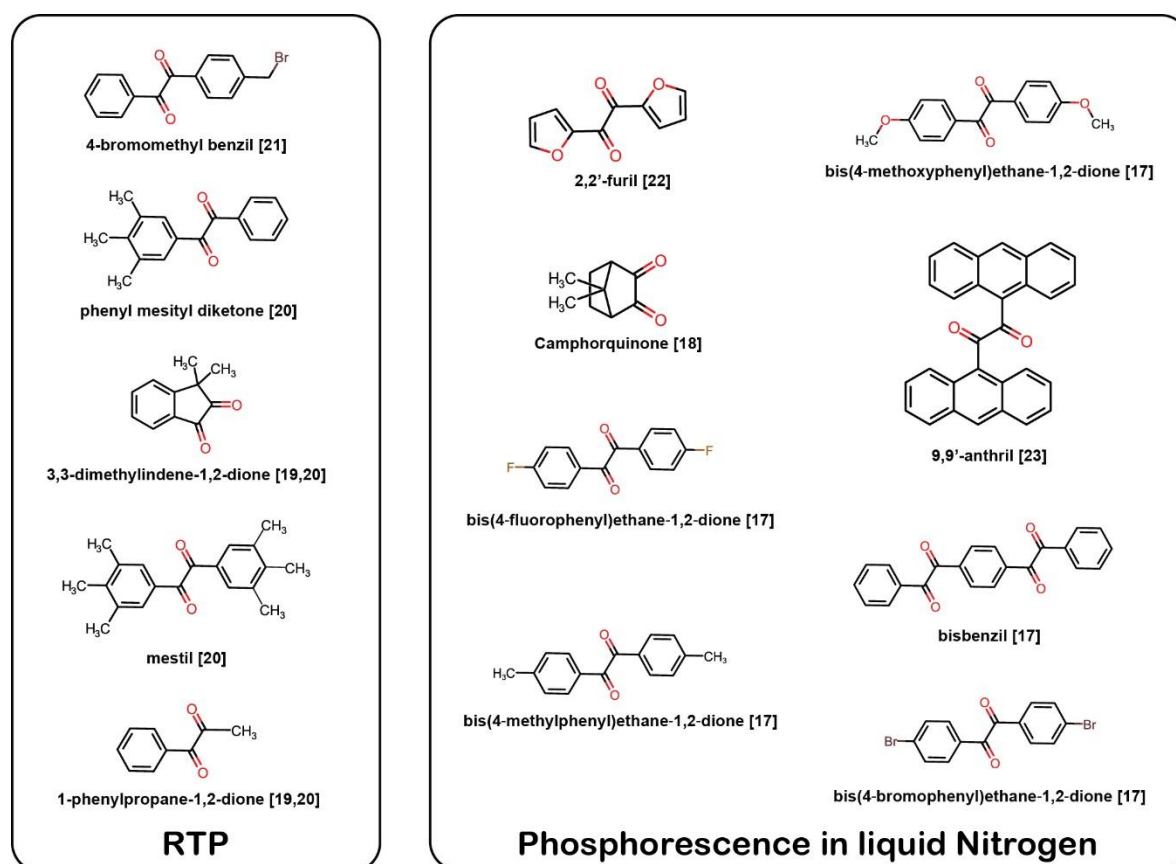


**Figure 1.**  $\alpha$ -Dicarbonyl molecules such as benzil and benzil derivatives reported to emit RTP or phosphorescence at 77 K.

Very recently, we reported the synthesis of new derivatives based on the benzil framework (Figure 2), as well as their steady-state photophysical properties [29]. Fluorinated monobenzil **1** and fluorinated (or non-substituted) bisbenzil **2** (and **3**), which are synthesised by a facile  $\text{PdCl}_2/\text{dimethyl}$

sulfoxide (DMSO) oxidation protocol from common bistolane derivatives, are capable of emitting RTP. The photoluminescence quantum yields (PLQYs) recorded for the derivatives in toluene solutions are approximately 2% for **1** and <1% for **2** and **3**. The absorption peaks at approximately 400 nm, which is the maximum absorption wavelength of the derivatives, are attributed to an  $n-\pi^*$  transition based on theoretical calculations. We determined that the fluorination of one side of the aromatic ring of the benzil derivatives may retard the ISC, leading to weaker RTP. In this study, we studied the excited-state dynamics of benzil derivatives using time-resolved PL spectroscopy to understand their photophysical properties. In addition, we investigated the photostability of **1–3** using a Xe flash lamp. The fundamental question is how do the side groups of the benzil derivatives affect the conformational flexibility and emission of RTP by comparison with benzil? In addition, we aimed to uncover the role of the monobenzil and bisbenzil structures, as well as the effect of the fluorination of the side group, on the low PLQY of these compounds.

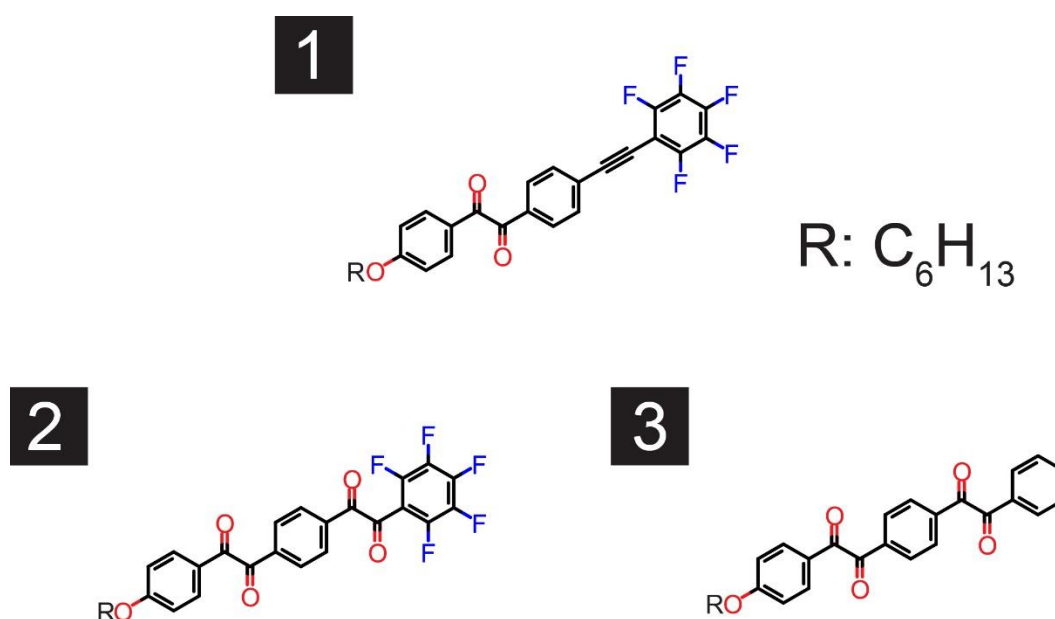


Figure 2. Benzil derivatives 1–3.

## 2. Materials and Methods

All benzils were synthesised from the corresponding bistolane derivatives following literature procedures [29] and were purified by column chromatography using a mixed solvent of hexane and EtOAc as an eluent, followed by recrystallisation from hexane before use. Spectroscopic grade toluene (FUJIFILM Wako Pure Chemical Corporation) was used as the solvent. Before preparing sample solutions, the water contaminating the solvents was removed using molecular sieves (105704, Merck). For all measurements, quartz cuvettes with 10-mm path length were used. To avoid the undesirable entry of ambient light, the sample cuvettes filled with the solutions were covered with aluminium foil. Steady-state ultraviolet-visible (UV-VIS) absorption spectra were obtained using a UV-3100 spectrometer (Shimadzu), whereas steady-state PL spectra were measured using a LS50B fluorescence spectrometer (Perkin Elmer) at an excitation wavelength of 290 nm via a Xe flash lamp with a long-path 320-nm filter set at the detection side. For time-resolved PL using single photon counting, we used a FluoroCube (Horiba). For the time-correlated single photon counting (TCSPC) method, a 342-nm pulsed laser diode (pulse width: 1 ns) was used, and for the multichannel scaler method (MCS) method, a 355-nm pulsed LED was used. In addition, the third-harmonic wavelength at 355 nm of a EKSPLA PL 2210 series diode-pumped picosecond kilohertz-pulsed Nd:YAG laser (pulse width 28 ps  $\pm$  10%) together with a 12-bit oscilloscope (Lecroy, Wavepro404HD) was used to measure the RTP lifetime. To measure the temperature-dependent PL spectra, sample solution cells were immersed directly in liquid N<sub>2</sub> or set in a liquid N<sub>2</sub> cryostat (Unisoku Co., Ltd., USP-203). The solution concentration was kept the

same for all samples. For N<sub>2</sub> purging of the sample solutions, pure N<sub>2</sub> gas (purity: 99.99995% (6N)) was used.

Theoretical calculations based on density functional theory (DFT) and time-dependent DFT (TD-DFT) were conducted for single molecules of **1–3** using the Gaussian 16 package. The optimised geometries of **1–3** were obtained for S<sub>0</sub> and S<sub>1</sub>. Using the S<sub>1</sub> geometry, the excitation energies of both S<sub>n</sub> and T<sub>n</sub> levels ( $n = 1-10$ ) were estimated. All calculations were performed at the M06-2X/6-31g(d) level of theory.

### 3. Results and discussion

#### 3.1. Photostability

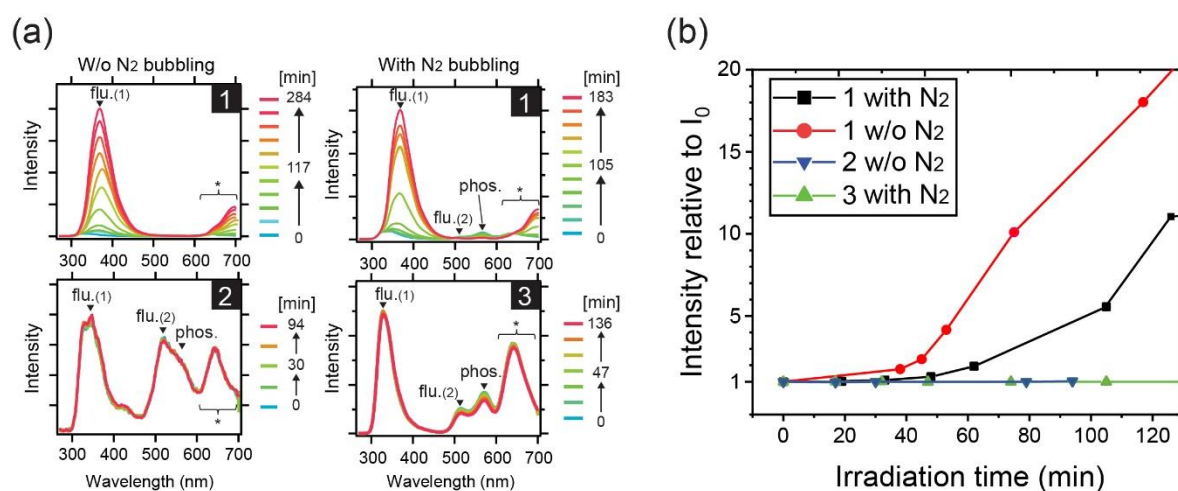


**Figure 3.** Photostability of **1–3** in toluene solutions. (a) Irradiation time dependence of PL spectra of **1–3** derivatives. The irradiations were conducted continuously to **1** and **2** solutions prepared w/o N<sub>2</sub> bubbling, and **1** and **3** solutions with N<sub>2</sub> bubbling. Asterisk (\*) is the region of second order diffracted light of flu.(1). (b) Time evolution of the intensity ratio at the peak of flu.(1) bands started from the initial peak intensity ( $I_0$ ).

First, we discuss the photostability of **1–3** in toluene based on steady-state measurements. Figure 3(a) shows the irradiation-time-dependent PL spectra of **1–3** in toluene obtained using a 290-nm Xe-flash lamp. Here, **1** was measured with and without (w/o) N<sub>2</sub> bubbling to investigate the photostability of both excited singlet and triplet states of the compound, respectively. For **2** and **3**, N<sub>2</sub> bubbling was performed only for **3** because both **2** and **3** showed similar PL patterns despite the presence of a fluorinated phenyl ring in **2**. The first fluorescence band (flu.(1)) peaked at 360–390 nm, the second fluorescence band (flu.(2)) peaked at approximately 520 nm, and the phosphorescence band (phos.) peaked at around 560 nm, as previously reported [29], and could be ascribed to an emission from S<sub>2</sub> for flu.(1), S<sub>1</sub> for flu.(2), and T<sub>1</sub> for phos. bands. These bands are typical of the benzil moiety [28, 30] but not toluene [31–35]. It is worth noting that we confirmed that the flu.(2) band is not a thermally activated delayed fluorescence band for **2**, as has been reported for benzil in imidazolium ionic liquids [27] (see Supplemental file and Figure S1). The absorption spectra of the fresh (irradiation time ( $t$ ) = 0 min) and the final sample of **1** solution are shown in Figure S2, where the initial absorbance of the maximum absorption band at approximately 313 nm decreased by 15% after the final PL measurement. Although the wavelength of the excitation light (290 nm) for the PL measurements is far from the absorption maximum wavelength at approximately 400 nm, 290-nm light was chosen to excite the molecules to higher excited singlet states, enabling the detection of both flu.(1) and flu.(2).

In Figure 3(a), it can be seen that the irradiation of **1** by light at the excitation wavelength caused a continuous change in the PL intensity, unlike **2** and **3**. For **1**, the flu.(2) and phos. bands observed after N<sub>2</sub> purging decreased in intensity, whereas flu.(1) gradually increases. The spectral change was

also observed irrespective of the N<sub>2</sub> purging, although the change was much less significant with N<sub>2</sub> purging. On the other hand, when the excitation wavelength was changed from 290 to 355 nm, there was a significant increase in the flu.(1) intensity of **1** over 486 min (Figure S3). Clearly, (**1**) **2** and **3** possess much higher photostability than **1**, and (**2**) the spectral change of **1** is most likely caused by a chemical reaction of the excited singlet states of **1**; otherwise, a stronger change would be expected to occur after N<sub>2</sub> purging owing to long-lived excited triplet states. For the reaction of **1**, the weakening of the flu.(2) and phos. bands, which are attributed to the n- $\pi^*$  transition of the benzil moiety, indicates chemical changes in the benzil portion. From the observation of the much higher photostability of **1** after irradiation with 355-nm light, it is suggested that the reaction occurs through higher excited singlet states. Usually, higher excited states, such as S<sub>2</sub> and T<sub>2</sub>, are rapidly deactivated via non-radiative routes to the corresponding lower excited states, that is, S<sub>1</sub> and T<sub>1</sub>, on a picosecond timescale, so-called Kasha's rule, and, thus, are less reactive. However, because RTP has been observed for **1-3**, the peculiar behaviour in the higher excited states is understandable and will be explained later in the time-resolved PL spectra.

### 3.2. Excited-state dynamics

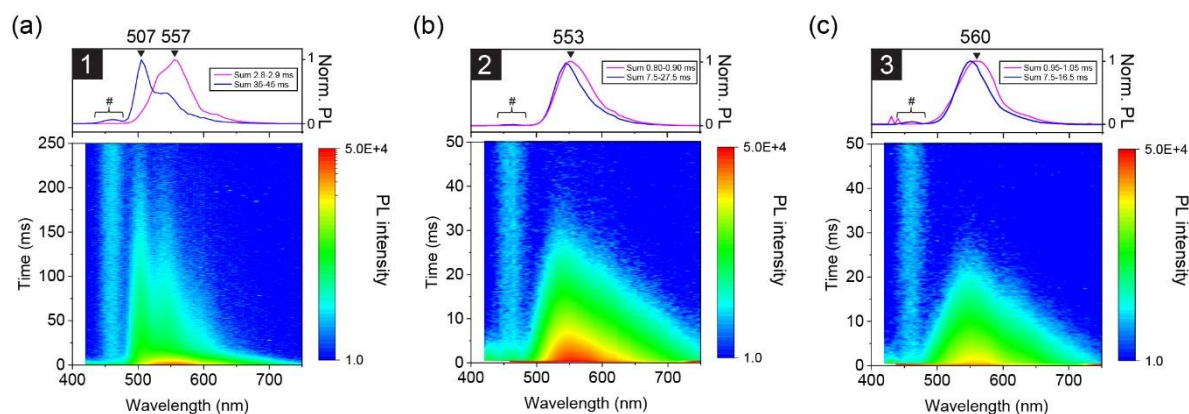


**Figure 4.** Time-resolved PL spectra of **1** (a), **2** (b), and **3** (c) at 77 K measured using the MCS method. The excitation light source was a pulsed light-emitting diode at 355 nm. The region marked with a hash (#) is a background feature attributed to scattering by the sample cell containing solvent.

After investigating the photostability of **1-3** in toluene, time-resolved PL measurements were performed; a negligible change in the absorption spectra after the measurements was confirmed. Figures 4(a) to 4(c) show time-resolved millisecond PL spectra of **1-3** in toluene measured at 77 K. Theoretical curve fitting was performed to estimate the time constant ( $\tau$ ) of the observed bands, and the results are summarised in Table S1. Initially, an intense band was observed at around 555 nm for all samples. The peak wavelength of the band for the three samples is matched to that of their RTP band, indicating the emission from T<sub>1</sub>. Subsequently, their PL spectra changed gradually. For **1**, an additional band appears at a shorter wavelength of 506 nm with vibronic progression. Similar behaviour has been reported for benzil in ethanol at 77 K [30]. The high-energy phosphorescence band was not observed for **2** and **3**, and it survived much longer than the T<sub>1</sub> band, and this was observed for all samples. These results indicate the existence of a higher excited triplet state for **1**, that is, T<sub>2</sub>. For **2** and **3**, only a slight narrowing of the initially observed T<sub>1</sub> emission band was identified. This can be explained by a uniform change in the molecular conformation distribution because the benzil moiety can twist during the relaxation process. Importantly, the lifetime of T<sub>2</sub> is longer than that of T<sub>1</sub>, meaning that the internal conversion (IC) from T<sub>2</sub> to T<sub>1</sub> is strongly suppressed at 77 K. Another point is that the peak position of the T<sub>2</sub> band is almost consistent with the S<sub>1</sub> band, that is, flu.(2) at room temperature, indicating a negligible energy gap (<0.01 eV) between S<sub>1</sub> and T<sub>2</sub>. This is supported by theoretical calculations, *vide infra*. The very small, almost negligible, gap leads us to expect a fast ISC for **1** between S<sub>1</sub> and T<sub>2</sub> according to the energy gap law.

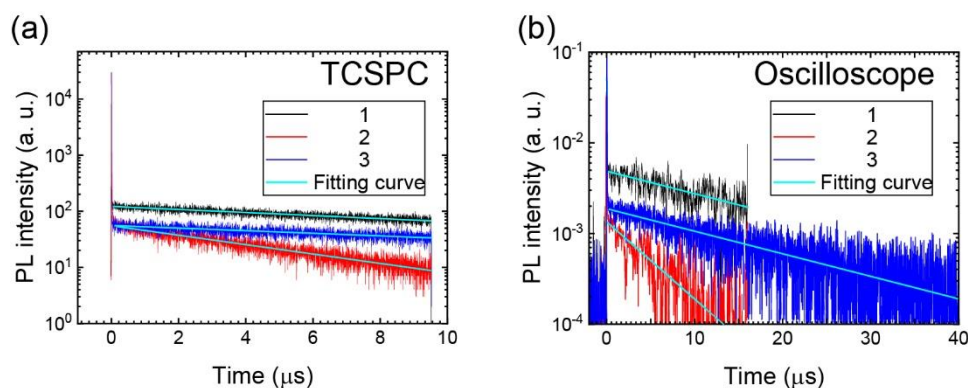


**Figure 5.** RTP lifetime measurements of **1–3** in solutions after  $N_2$  purging using (a) TCSPC and (b) 12-bit oscilloscope.

The observation of a longer  $T_2$  lifetime compared to that of  $T_1$  at 77 K (Figure 4(a)) implies anti-Kasha behaviour in **1** [36]. This suggests that **1** shows different RTP behaviour to those of **2** and **3**. However, we characterised the RTP time profiles under nearly identical absorbance conditions for the excitation light, so the existence of  $T_2$  in **1** affects the ISC efficiency but not the RTP lifetime. Figures 5(a) and 5(b) show the transient PL results of the RTP band measured by TCSPC and a 12-bit oscilloscope, respectively. The former was conducted first and the latter was performed to confirm the TCSPC data because our TCSPC systems had difficulty measuring the measurement time region with sufficient time resolution for **1** and **3**. A single decay exponential function was successfully used for curve fitting of the time profiles of both the measurement systems;  $\tau$  of RTP ( $\tau_{RTP}$ ) was estimated to be 16.9  $\mu s$  (by TCSPC)/17.5  $\mu s$  (by oscilloscope) for **1**, 5.2  $\mu s$ /5.2  $\mu s$  for **2**, and 18.8  $\mu s$ /17.5  $\mu s$  for **3**. Compounds **1** and **3** exhibit relatively large and very similar  $\tau_{RTP}$  values compared to **2**. Because **2** and **3** only differ by the substituted F atoms on the phenyl side group, we inferred that fluorination may decrease the RTP lifetime. The amplitude of **1** is stronger than **3** by a factor of 3.6, but the lifetimes are very similar. This implies a faster ISC in **1** than **3**, plausibly because  $T_2$  is very close to  $S_1$ . The small difference in the amplitude between **2** and **3**, which differ by a factor of 1.4, suggests a similar ISC process for the two derivatives, but the  $T_1$  lifetime is longer for **3** than **2**, which results in a more intense RTP emission in non-fluorinated **3**.

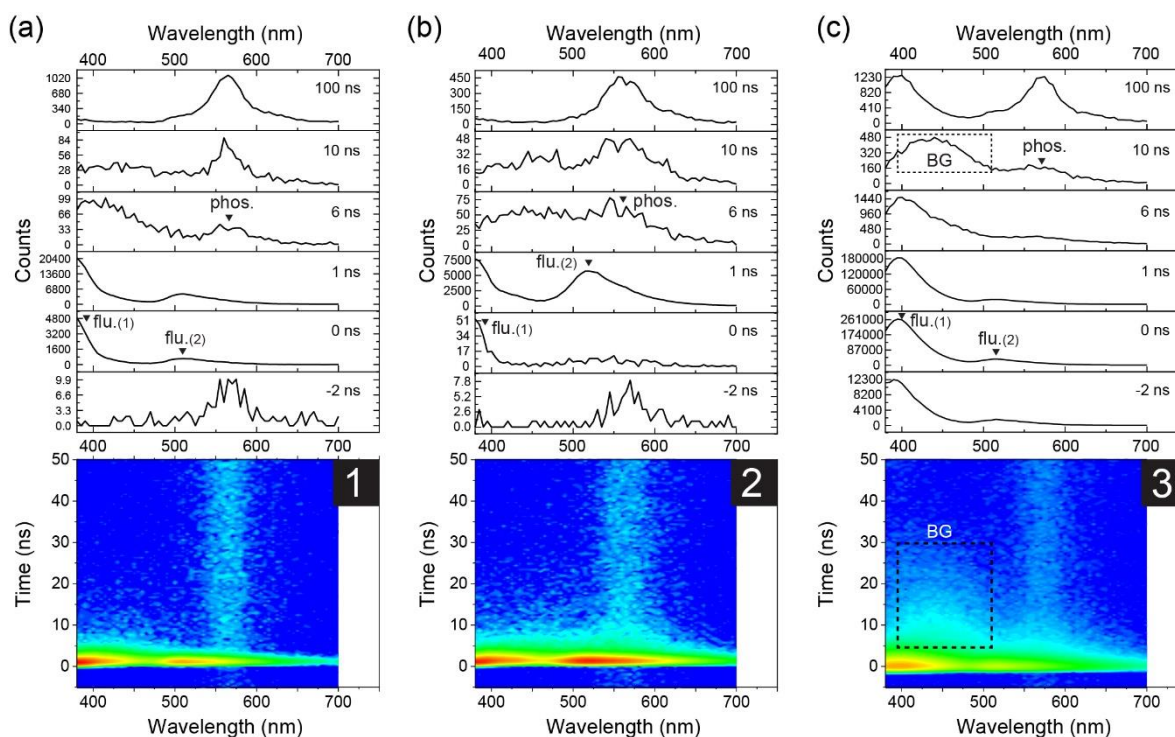


**Figure 6.** Time-dependent PL spectra of **1** (a), **2** (b), and **3** (c) in toluene solutions with N<sub>2</sub> bubbling measured by TCSPC. The square region with the broken line, denoted BG (background), in (c) is the scattered light from the sample solutions.

Finally, we present the room-temperature time-resolved nanosecond PL spectra of **1–3** in toluene. The TCSPC spectral data in Figures 6(a)–6(c) show the simultaneous decay of flu.(1) and flu.(2) for **1–3**. This anomalous result suggests that IC from S<sub>2</sub> to S<sub>1</sub> and radiative decay from S<sub>2</sub> to S<sub>0</sub> are competitive processes for **1–3**, unlike non-RTP compounds. Because of the limited time resolution of our apparatus, we could not distinguish the IC process from the data, that is, the decrease in S<sub>2</sub> and increase in S<sub>1</sub>, implying that S<sub>1</sub> decays very fast compared to S<sub>2</sub>, and the IC restricts the decay time of S<sub>1</sub>. The values of  $\tau$  for the flu.(1) and flu.(2) peaks estimated by curve fitting (see Figure S5) are similar for each compound, but there is a chemical structure dependence;  $\tau$  is shorter in order of **1** (0.48 ns) < **2** (0.56–0.67 ns) < **3** (0.79–0.95 ns). Note that the value of 0.48 ns is almost the same as the  $\tau$  of scattered light of the excitation light pulse of 0.45 ns, indicating that the present  $\tau$  of **1** may be the upper limit. Remarkably, the  $\tau$  of **1** is significantly shorter than that of **3**, despite their similar  $\tau_{\text{RTP}}$  values, as discussed in the previous section. These results imply that the fluorination at the side phenyl group of the benzil framework controls the radiative decay of the singlet excited state (but not ISC) to the excited triplet state. Again, the ISC rate of **1** is different from those of the others because of presence of the T<sub>2</sub> state.

As mentioned in the introduction, excited  $\alpha$ -dicarbonyl derivatives have been reported to be photoisomerised from a cis-skewed geometry in S<sub>0</sub> to a TP geometry in excited S and T states [30]. However, a recent work by Bhattacharya et al. revealed that, depending on the excitation wavelength, emission from S<sub>1</sub> and S<sub>2</sub> can be attributed to the skewed form of benzil, whereas S<sub>1</sub> also fluoresces from the TP conformer [28]. In the present study, the observation of both S<sub>1</sub> (flu.(2)) and S<sub>2</sub> (flu.(1)) emissions suggests that the geometries of **1–3** in the excited single state are cis-skewed or cis-skewed-like, which is not a perfect TP geometry. Further, Roy et al. studied the emissions of benzil in ethanol solution at 77 K and observed a phosphorescence peak at around 530 nm. Upon increasing the temperature (to just below the melting point), a second phosphorescence band emerged at approximately 570 nm, which was ascribed to the emission originating from a coplanar (TP) geometry of the excited triplet state that grows by the relaxation of the skew geometry in the excited triplet state. Based on this result, we could expect that the TP geometry is formed in **1–3** at 77 K and room temperature, but only **1** can simultaneously maintain the unrelaxed skew geometry at 77 K.

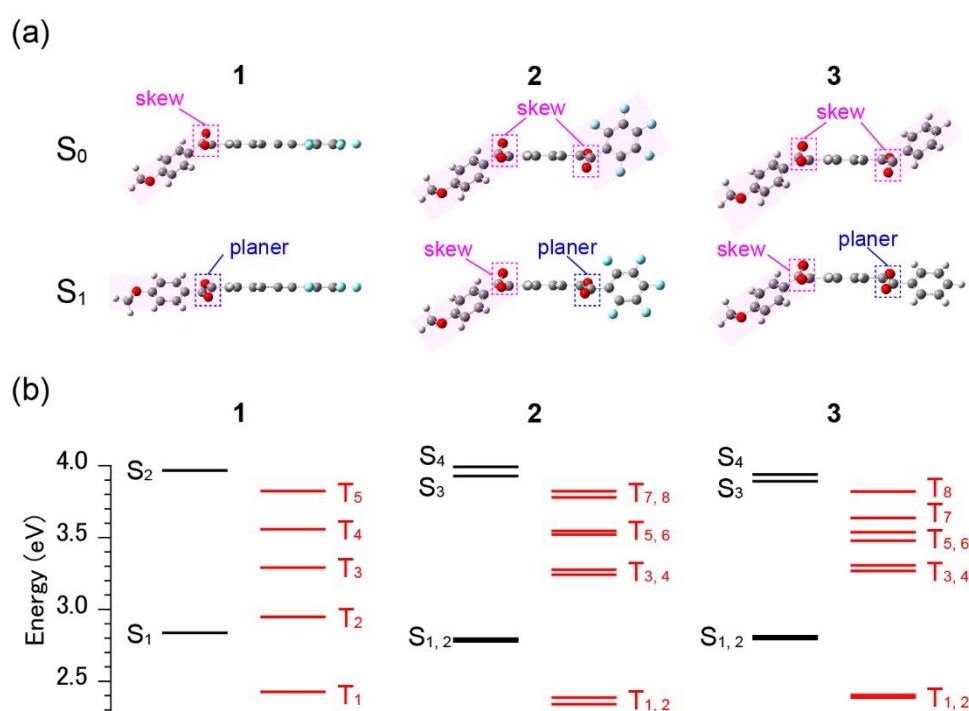


**Figure 7.** Theoretical calculations for 1–3. (a) Optimised conformations at the  $S_1$  and  $S_1$  levels. (b) Energy level diagram of some excited  $S_n$  and  $T_n$  levels. All calculations were conducted at the M06-2X/6-31g(d) level of theory.

To verify the above hypotheses, we conducted theoretical calculations of 1–3 using DFT and TD-DFT. Figure 7(a) shows the molecular geometries of 1–3 optimised for  $S_0$  and  $S_1$  states. All the derivatives exhibit a skew geometry of the benzil moieties in  $S_0$ . Owing to the skew geometry, the side phenyl groups are significantly bent away from the plane of the central phenyl rings (see the pink square in Figure 7(a)). In the  $S_1$  geometry, on the other hand, the conformation of the dicarbonyl group is more planar in 1 and the side phenyl ring is close to the plane of the central phenyl ring. For 2 and 3, the geometries of the  $S_1$  states are the same as for 1, only the dicarbonyl group connected to the other side of the phenyl with no alkoxy group becomes planar: the geometry of other dicarbonyl groups with alkoxy phenyl rings remains unchanged. A close inspection of 2 reveals that the planarity of the side perfluorinated phenyl ring relative to the central phenyl ring is lower than that of the non-substituted phenyl ring of 3. This is an effect of the greater steric bulk of 2 compared to 3.

In contrast, there are distinct differences in the energy level diagram in Figure 7(b). In Figure 7(b), only 1 possesses a  $T_2$  level in the vicinity of  $S_1$  (separation of approximately 0.1 eV). For 2 and 3, the  $T_2$  levels are very close to  $T_1$ , which is approximately 0.4 eV below  $S_1$ . Further, the next  $T_3$  level is also above  $S_1$  by the same value. As previously mentioned, the close vicinity of  $T_2$  to  $S_1$  was expected for 1 alone based on the time-resolved PL spectra measured at 77 K shown in Figure 4(a). This supports our consideration that fast ISC occurs only for 1 according to the energy gap law because, for 2 and 3, there is no  $T_n$  level close to  $S_1$  and the energy gap between  $S_1$  and  $T_1$  is the same (approximately 0.4 eV) for all derivatives. The latter fact, where  $S_1$  and  $T_1$  have energies within < 0.05 eV for the three derivatives, is consistent with the fluorescence and phosphorescence spectra and their dynamics, which are not drastically different for 1–3.

Finally, we discuss the correlation between the dynamics and PLQY of 1–3. Previously, we reported that the PLQY of 1 in toluene measured after  $N_2$  purging was 1.8%, whereas those of 2 and 3 under the same conditions were less than 1%. These results indicate that most of the excited states of 1–3 are deactivated non-radiatively to  $S_0$ . In this sense, the high PL efficiency, particularly, the high RTP efficiency, must result from the strong suppression of the non-radiative decay process. The fact that RTP is observable because of the fast ISC (< 1 ns) suggests that the excited singlet states are mostly converted to excited triplet states. This is similar to, for example, the nearly 100% triplet yield efficiency from the excited singlet state for benzophenone, whose ISC rate constant has been reported to be 9 to 16 ps<sup>-1</sup> in solution [37]. Benzil has also been reported to have  $\tau$  in the sub-picosecond to several tens-of-picoseconds regime in various solvents [23] and have a high triplet yield of 0.92 (in solid form) [28]. For 1–3, it is likely that the decrease in conformational flexibility at the dicarbonyl group suppresses the ISC rate compared to only a benzil. This is obvious for 2 and 3, whose bulky substituents on one side of the benzil moiety restrict the twisting motion of the other side of the benzil moiety, which reduces further their slow ISCs compared to that of 1. The role of fluorination of one side of the phenyl group connected to benzil is not clear at this moment. However, fluorination does not seem to help enhance the ISC or strengthen the PLQY, although the F atom is certainly heavier than the H atom. Therefore, the electronic effect of the F atom on the bisbenzil framework is not significant; in other words, the heavy metal effect does not apply to the derivatives. Probably, the conformational change in excited triplet states should be considered because a clear change in conformation from the  $S_1$  state to the ground triplet state was observed only for 2 by theory (Figure S6). To understand this further, the direct estimation of excited triplet states by transient absorption spectroscopy, as well as determination of the proper decay constant of excited singlet states, which was limited in the present study because of the insufficient time resolution of our apparatus, is required.

#### 4. Conclusions

We investigated the excited state dynamics and photostability of monobenzil and bisbenzil derivatives (1–3) in toluene. Monobenzil derivative **1** exhibited strong degradation upon irradiation with 290-nm light. Time-resolved PL studies uncovered the following findings.

- (1) The lifetime of RTP for the present benzil derivatives is the microsecond regime.
- (2) The monobenzil derivative possesses a longer lifetime and more intense RTP emission than the bisbenzil derivatives.
- (3) Fluorination at one side of the phenyl groups of benzil does not significantly affect the behaviour of the excited triplet state but shortens the lifetime of the excited singlet state.

From the experimental and theoretical results, the distinct characteristics of the monobenzil derivative can be explained by the T<sub>2</sub> state having almost the same energy as S<sub>1</sub>. For efficient RTP materials containing a benzil framework, the attachment of bulky substituents may be undesirable because it suppresses the conformational flexibility at the dicarbonyl portion, which is key to the efficient ISC of benzil derivatives.

**Supplementary Materials:** The following are available online at [www.mdpi.com/xxx/s1](http://www.mdpi.com/xxx/s1), Figure S1: Temperature dependence of PL spectra of **2** after N<sub>2</sub> bubbling, Figure S2: Absorptions spectra of **1** in toluene solution with N<sub>2</sub> bubbling: Before and after irradiation of Xe-290 nm light shown in Figure 3(a), Figure S3: (a) Photostability of **1** in toluene solutions with N<sub>2</sub> bubbling using Xe-355 nm lamp. (b) The ratio of peak intensity of flu.(1) band (*I*<sub>t</sub>) to the initial peak intensity (*I*<sub>0</sub>). Figure S4: Triple decay emission at 77 K of **1** – **3** in toluene solutions. The peaks are chosen from Fig. 4 in the main text. Figure S5: Time profiles of flu. (1), flu. (2) and phos. bands of **1** – **3** in toluene solutions taken from Fig. 5.: flu. (1) is 380 nm for **1** and **2**, 400 nm for **3**, flu. (2) is 508 nm for **1**, 518 nm for **2**, and 522 nm for **3**, phos. is 606 nm for **1**, 558 nm for **2**, and 582 nm for **3**, respectively. Figure S6: Optimized structure of **1** – **3** in the ground triplet state obtained by DFT calculations [M06-2X/6-31g(d)]. Table S1: Amplitudes (*A<sub>n</sub>*) and time constants (*τ<sub>n</sub>*) estimated by theoretical curve fittings of time-profiles of PL spectra of **1** – **3** in toluene solutions measured at 77 K.

**Author Contributions:** Conceptualization, T.H., K.M., and S.Y.; methodology, K.M., S.Y., and T.H.; formal analysis, K.M., and T.H.; investigation, K.M., S.Y., and T.H.; resources, S.Y., and T.K.; writing—original draft preparation, K.M., and T.H.; writing—review and editing, T.H., K.M., K.K., S.Y., and T.K.; supervision, T.K., K.K., and T.H.; funding acquisition, T.H. All authors have read and agreed to the published version of the manuscript.

**Funding:** This work was partly supported by the Japan Society for the Promotion of Science (JSPS) KAKENHI Grant-in-Aid for Scientific Research (C) (Grant No. JP18K05267 and JP18H03902) and the AIST Nanocharacterization Facility (ANCF) platform as a part of a program of the ‘Nanotechnology Platform’ of the Ministry of Education, Culture, Sports, Science and Technology (MEXT), Japan.

**Acknowledgments:** We sincerely thank Mr. Takuya Higashida for the synthesis of the fluorinated monobenzil and bisbensils, and Ms. Minori Furukori for the edition of this manuscript. We would like to thank Editage ([www.editage.com](http://www.editage.com)) for English language editing.

**Conflicts of Interest:** The authors declare no conflict of interest.

## References

1. Baldo, M. A.; O'Brien, D. F.; You, Y.; Shoustikov, A.; Sibley, S.; Thompson, M. E.; Forrest, S. R., Highly efficient phosphorescent emission from organic electroluminescent devices. *Nature* **1998**, *395*, 151–154.
2. Diaz-Garcia, M. E.; Fernandez-Gonzalez, A.; Badia-Laino, R., The triplet state: Emerging applications of room temperature phosphorescence spectroscopy. *Appl. Spectrosc. Rev.* **2007**, *42*, 605–624.
3. Haneder, S.; Da Como, E.; Feldmann, J.; Lupton, J. M.; Lennartz, C.; Erk, P.; Fuchs, E.; Molt, O.; Munster, I.; Schildknecht, C.; Wagenblast, G., Controlling the radiative rate of deep-blue electrophosphorescent organometallic complexes by singlet-triplet gap engineering. *Adv. Mater.* **2008**, *20*, 3325–3330.
4. Wu, W.; Sun, J.; Cui, X.; Zhao, J., Observation of the room temperature phosphorescence of Bodipy in visible light-harvesting Ru(II) polyimine complexes and application as triplet photosensitizers for triplet-triplet-annihilation upconversion and photocatalytic oxidation. *J. Mater. Chem. C* **2013**, *1*, 4577–4589.
5. Fateminia, S. M. A.; Mao, Z.; Xu, S.; Yang, Z.; Chi, Z.; Liu, B., Organic Nanocrystals with Bright Red Persistent Room-Temperature Phosphorescence for Biological Applications. *Angew. Chem. Int. Ed.* **2017**, *56*, 12160–12164.

6. Jiang, K.; Wang, Y.; Cai, C.; Lin, H., Conversion of Carbon Dots from Fluorescence to Ultralong Room-Temperature Phosphorescence by Heating for Security Applications. *Adv. Mater.* **2018**, *30*, e1800783(1–8).
7. Green, D. C.; Holden, M. A.; Levenstein, M. A.; Zhang, S.; Johnson, B. R. G.; Gala de Pablo, J.; Ward, A.; Botchway, S. W.; Meldrum, F. C., Controlling the fluorescence and room-temperature phosphorescence behaviour of carbon nanodots with inorganic crystalline nanocomposites. *Nat. Commun.* **2019**, *10*, 206(1–13).
8. Bilen, C. S.; Harrison, N.; Morantz, D. J., Unusual Room-Temperature Afterglow in Some Crystalline Organic-Compounds. *Nature* **1978**, *271*, 235–237.
9. Hirata, Y.; Lim, E. C., Nonradiative Electronic Relaxation of Gas-Phase Aromatic Carbonyl-Compounds - Benzaldehyde. *J. Chem. Phys.* **1980**, *72*, 5505–5510.
10. Donkerbroek, J. J.; Elzas, J. J.; Gooijer, C.; Frei, R. W.; Velthorst, N. H., Some Aspects of Room-Temperature Phosphorescence in Liquid Solutions. *Talanta* **1981**, *28*, 717–723.
11. Yuan, W. Z.; Shen, X. Y.; Zhao, H.; Lam, J. W. Y.; Tang, L.; Lu, P.; Wang, C. L.; Liu, Y.; Wang, Z. M.; Zheng, Q.; Sun, J. Z.; Ma, Y. G.; Tang, B. Z., Crystallization-Induced Phosphorescence of Pure Organic Luminogens at Room Temperature. *J. Phys. Chem. C* **2010**, *114*, 6090–6099.
12. Kwon, M. S.; Yu, Y.; Coburn, C.; Phillips, A. W.; Chung, K.; Shanker, A.; Jung, J.; Kim, G.; Pipe, K.; Forrest, S. R.; Youk, J. H.; Gierschner, J.; Kim, J., Suppressing molecular motions for enhanced room-temperature phosphorescence of metal-free organic materials. *Nat. Commun.* **2015**, *6*, 8947(1–9).
13. Hirata, S., Recent Advances in Materials with Room-Temperature Phosphorescence: Photophysics for Triplet Exciton Stabilization. *Adv. Opt. Mater.* **2017**, *5*, 1700116(1–50).
14. Li, D.; Lu, F.; Wang, J.; Hu, W.; Cao, X. M.; Ma, X.; Tian, H., Amorphous Metal-Free Room-Temperature Phosphorescent Small Molecules with Multicolor Photoluminescence via a Host-Guest and Dual-Emission Strategy. *J. Am. Chem. Soc.* **2018**, *140*, 1916–1923.
15. Zhan, G.; Liu, Z.; Bian, Z.; Huang, C., Recent Advances in Organic Light-Emitting Diodes Based on Pure Organic Room Temperature Phosphorescence Materials. *Front. Chem* **2019**, *7*, 305(1–6).
16. Morantz, D. J.; Wright, A. J. C., Structures of the Excited States of Benzil and Related Dicarboxyl Molecules. *J. Chem. Phys.* **1971**, *54*, 692–697.
17. Gong, Y. Y.; Tan, Y. Q.; Li, H.; Zhang, Y. R.; Yuan, W. Z.; Zhang, Y. M.; Sun, J. Z.; Tang, B. Z., Crystallization-induced phosphorescence of benzils at room temperature. *Sci. China-Chem.* **2013**, *56*, 1183–1186.
18. Tsai, L.; Charney, E., The triplet states of alpha-dicarbonyls. Camphorquinone. *J. Phys. Chem.* **1969**, *73*, 2462–3.
19. Arnett, J. F.; Newkome, G.; Mattice, W. L.; McGlynn, S. P., Excited electronic states of the  $\alpha$ -dicarbonyls. *J. Am. Chem. Soc.* **1974**, *96*, 4385–4392.
20. Arnett, J. F.; McGlynn, S. P., Phototautomerism of Aromatic Alpha-Dicarbonyls. *J. Phys. Chem.* **1975**, *79*, 626–629.
21. Gebert, M. S.; Torkelson, J. M., Synthesis, Characterization and Photophysical Properties of Benzil-Labeled Polymers for Studies of Diffusion-Limited Interactions by Phosphorescence Quenching. *Polymer* **1990**, *31*, 2402–2410.
22. Singh, A. K.; Palit, D. K., Excited-state dynamics and photophysics of 2,2'-furyl. *Chem. Phys. Lett.* **2002**, *357*, 173–180.
23. Singh, A. K.; Palit, D. K.; Mittal, J. P., Conformational relaxation dynamics in the excited electronic states of benzil in solution. *Chem. Phys. Lett.* **2002**, *360*, 443–452.
24. Kundu, P.; Chattopadhyay, N., Photophysics of Anthril in Fluids and Glassy Matrixes. *J. Phys. Chem. A* **2018**, *122*, 5545–5554.
25. Miyasaka H., M. N. I. H. C. B., Ippen E.P., Mourou G.A., Zewail A.H. (eds) Ultrafast Phenomena VII. Springer Series in Chemical Physics, vol 53. Springer, Berlin, Heidelberg, Femtosecond Laser Photolysis Studies on the Conformation Change of Benzil in Solutions.
26. Ikeda, N.; Koshioka, M.; Masuhara, H.; Yoshihara, K., Picosecond Dynamics of Excited Singlet-States in Organic Microcrystals - Diffuse Reflectance Laser Photolysis Study. *Chem. Phys. Lett.* **1988**, *150*, 452–456.
27. Khara, D. C.; Samanta, A., Fluorescence, Phosphorescence, and Delayed Fluorescence of Benzil in Imidazolium Ionic Liquids. *Aust. J. Chem.* **2012**, *65*, 1291–1297.
28. Bhattacharya, B.; Jana, B.; Bose, D.; Chattopadhyay, N., Multiple emissions of benzil at room temperature and 77 K and their assignments from ab initio quantum chemical calculations. *J. Chem. Phys.* **2011**, *134*, 044535(1–7).

29. Yamada, S.; Higashida, T.; Wang, Y.; Morita, M.; Hosokai, T.; Maduwantha, K.; Koswattage, K. R.; Konno, T., Development of fluorinated benzils and bisbenzils as room-temperature phosphorescent molecules. *Beilstein J. Org. Chem.* **2020**, *16*, 1154–1162.
30. Roy, D. S.; Bhattacharyya, K.; Bera, S. C.; Chowdhury, M., Conformational relaxation in the excited electronic states of benzil and naphthyl. *Chem. Phys. Lett.* **1980**, *69*, 134–140.
31. Hirata, Y., Photophysical and photochemical primary processes of diphenylacetylene derivatives and related compounds in liquid phase. *Bull. Chem. Soc. Jpn.* **1999**, *72*, 1647–1664.
32. Wahadoszamen, M.; Hamada, T.; Iimori, T.; Nakabayashi, T.; Ohta, N., External electric field effects on absorption, fluorescence, and phosphorescence spectra of diphenylpolyynes in a polymer film. *J. Phys. Chem. A* **2007**, *111*, 9544–9552.
33. Menning, S.; Kramer, M.; Coombs, B. A.; Rominger, F.; Beeby, A.; Dreuw, A.; Bunz, U. H., Twisted tethered tolanes: unanticipated long-lived phosphorescence at 77 K. *J. Am. Chem. Soc.* **2013**, *135*, 2160–2163.
34. Agneeswari, R.; Tamilavan, V.; Hyun, M. H., Synthesis and Characterization of 1,2,4-Oxadiazole-Based Deep-Blue and Blue Color Emitting Polymers. *Bull. Korean Chem. Soc.* **2014**, *35*, 513–517.
35. Kramer, M.; Bunz, U. H.; Dreuw, A., Comprehensive Look at the Photochemistry of Tolane. *J. Phys. Chem. A* **2017**, *121*, 946–953.
36. Zhou, Y.; Baryshnikov, G.; Li, X.; Zhu, M.; Ågren, H.; Zhu, L., Anti-Kasha's Rule Emissive Switching Induced by Intermolecular H-Bonding. *Chem. Mater.* **2018**, *30*, 8008–8016.
37. Katoh, R.; Kotani, M.; Hirata, Y.; Okada, T., Triplet exciton formation in a benzophenone single crystal studied by picosecond time-resolved absorption spectroscopy. *Chem. Phys. Lett.* **1997**, *264*, 631–635.